IMPROVEMENTS IN SLS PART ACCURACY

Christian Nelson
Kevin McAlea
Damien Gray
DTM Corporation
Austin, Texas 78754

ABSTRACT

SLS® part accuracy is influenced by a number of machine and material characteristics. Some of the most significant sources of error are associated with laser beam positioning (static and dynamic) on the part bed surface and uncertainty in the calibration factors used to compensate for material shrinkage and growth as well as the finite width of the laser beam. Another source of error is the minimum resolution of the process, which is a dependent on the particle size and shape of the material. In this presentation, technical background on these issues will be provided. In addition, part data obtained with a number of SLS materials demonstrating improved accuracy obtained through machine modifications and improved calibration methods will be described.

1. INTRODUCTION

Rapid prototyping part accuracy has been reported in a number of studies. In the case of stereolithography, a large amount of accuracy data has been generated for a model geometry to characterize process and material technology improvements over time (1, 2). More recently, a number of studies which compare the accuracy of different rapid prototyping technologies have been documented (3-6). In nearly all of these studies, accuracy has been reported as the deviation of measured dimensions from the desired dimensions. Other components of accuracy are also important to users of these technologies. In particular, trueness of features as characterized by the sharpness of corners and edges and detail resolution is quite important. as is the ease of part fit and assembly. In this study, improvements in the accuracy of SLS parts as characterized by both dimensional tolerances and trueness of features will be discussed. In addition, a discussion of critical material and process issues which affect accuracy will be provided.

2. BACKGROUND

2.1 The SLS Process A schematic of the SLS process as commercialized by DTM is shown in Figure 1. The key components are a CO_2 laser, laser optics and scanning mirrors, part build cylinder, feed cartridges, heaters, and a roller mechanism. To fabricate a part, powder from one of the feed cartridges is first spread in a thin, uniform layer over the part bed surface. A typical layer thickness is 0.12 mm. The laser beam is rastered over the part bed surface with the scanning mirrors and the laser energy modulated so that only the area which corresponds to the cross section of the object is fused. The 2D cross sections are defined by software which "slices" the 3D CAD information into layers. A new layer of powder is then spread from the other feed

cartridge, the new layer scanned with the laser, and this process repeated until the part is complete. Sufficient laser energy is used so that each new layer is bonded to the previous layer. As the part is fabricated, the unfused powder provides support for features such as overhangs. After the build is complete, this unfused powder can typically be blown or brushed off the part. The temperatures of part and feed powders are independently controlled with radiant heaters in order to minimize the development of thermal stresses in parts and prevent warpage. The part bed temperature is typically held just below the softening or melting point of the material, while the feed bed temperature is held at a low enough temperature so the powder remains free flowing and can be spread by the roller.

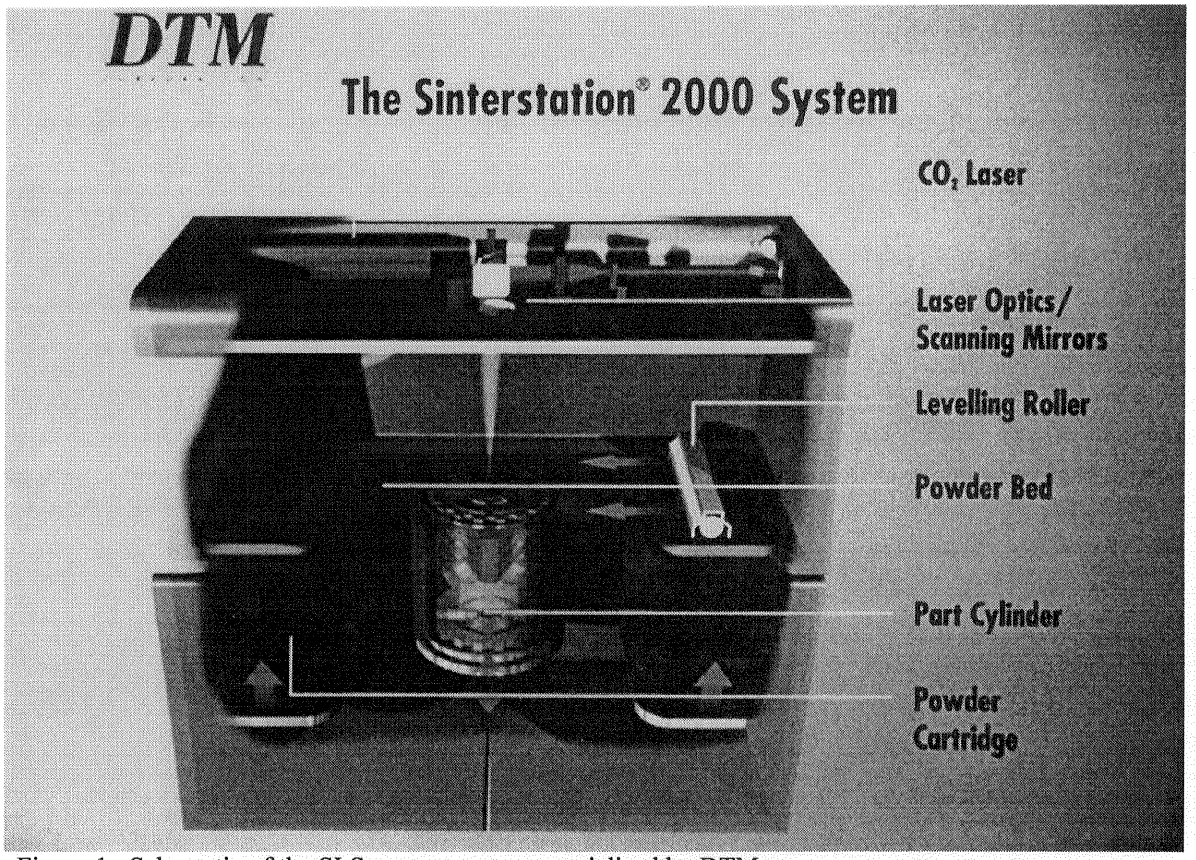

Figure 1. Schematic of the SLS process as commercialized by DTM.

2.2 Accuracy - Material Effects Melting/softening behavior and particle size and shape are two key material properties which affect part accuracy. The melting/softening behavior of materials affects part density, shrinkage, and the sintering of powder outside the desired part boundaries, or "growth". Growth is caused by heat transfer from the consolidated part to the surrounding support powder. The relationship between melting/softening behavior and part density has been discussed previously (7). Materials with a broad softening range (amorphous systems) are typically processed with relatively high laser powers and yield less than full density parts, while materials with sharp melting transitions (crystalline or semicrystalline systems) are typically processed with lower laser powers and can yield near full density parts. The limited consolidation obtained with amorphous systems results in relatively low shrinkage (typically about 1%), but the relatively high laser powers which are used to make the parts can cause

considerable growth. Crystalline or semicrystalline materials exhibit high shrinkage (typically 3-4%) associated with both the material phase change and the high degree of consolidation obtained during processing, but the amount of growth is usually limited by the relatively low laser powers which are required to completely melt the material. While software is used to compensate for the dimensional changes associated with material shrink and growth, the best accuracy is usually obtained when these compensations are small. For a given material, it is possible to moderate shrink and growth by adding a reinforcement or filler to the system (8, 9). It is also possible to achieve near zero shrinkage with multiphase coated particle morphologies (10, 8).

The primary effect of particle size and shape on part accuracy is on the trueness of features. Smaller particles with a high degree of sphericity produce parts with sharper edges and corners and improved detail resolution. In addition, the layer thickness of parts can be reduced for smaller particle sizes which reduces the "stair step" effect which is common to all layered manufacturing processes.

2.3 Accuracy - Process Effects The key process elements which affect part accuracy are the beam delivery and thermal control systems. As previously described, the beam delivery system uses scanning mirrors to position the laser beam on the part bed surface. There are errors associated with the inherent positional accuracy of the scanning system as well as dynamic errors associated with coordinating the laser "on" and "off" with the acceleration and deceleration of the mirrors. This type of dynamic error causes scan vectors to be drawn with a non-uniform energy density. In addition, the finite size of the laser beam causes material outside the part boundaries to be scanned. Part dimensions are adjusted for the finite diameter of the beam through a software compensation, just as they are for growth. From a practical standpoint, the effects of growth and finite beam diameter on part accuracy are indistinguishable since they both cause a constant increase in part dimensions.

Adequate thermal control is necessary to prevent accuracy problems associated with part warpage or "curl". Warpage can occur at the part bed surface or "in-build", or as the part is cooled from the build temperature to room temperature or "post-build". In-build curl is caused by thermal stresses and layerwise shrinkage stresses. These stresses can be minimized by maintaining the part bed at a temperature near the melting/softening temperature of the material. At this temperature, thermal gradients between the part and surrounding powder are minimized while for viscoelastic materials such as polymers, stress relaxation is activated. Post-build curl is caused by stresses which develop as the result of non-uniform part cooling. This mechanism is particularly important for high temperature materials. The control of post-build curl through cooling rate control has been previously described (7, 11). An additional thermal accuracy issue can result from point-to-point temperature differences in a consolidated part. Temperature variability is caused by non-uniform power densities experienced by different cross-sections as the laser is scanned across a part geometry. This thermal variability can cause non-uniform shrinkage and growth. Temperature feedback control techniques for eliminating these effects have been discussed (12).

The current work is focused on three of the accuracy elements described above: scanning dynamics, scale/offset calibration and compensation software, and particle size and shape control. Improvements in these areas are described.

3. IMPROVEMENTS

3.1.1 Scanner Dynamics Inherent with any scanning system are errors associated with the positional accuracy and dynamics of the galvanometers. The magnitude of the errors is affected by the mass of the mirrors and manufacturers design. The dynamic error is defined as the error that results from exceeding the bandwidth of the system, where the bandwidth is how fast the system can accurately respond to changes. The impact of dynamic errors on part accuracy can be reduced by slowing down the scan speed, minimizing the mass of the galvanometer mirrors, or changing the design of the galvanometers. DTM is currently evaluating a set of experimental galvanometers with different design parameters than the current galvanometers.

Dynamic errors were measured in a machine using a simple test where two series of marks are burnt onto a sheet of Mylar. The first series is drawn at a slow scan speed (0.86 m/s), and the second set is drawn at a fast scan speed (2.36 m/s). The marks made at the slow scan speed are used as a reference from which the second series of marks is measured. The dynamic error is the difference between the actual and the ideal position of the marks drawn at the fast scan speed. The dynamic errors measured for the current and experimental galvanometers are ± 0.25 and ± 0.025 millimeters, respectively, as shown in Figure 2. The results of this test show that the galvanometer design plays an important role in dynamic performance.

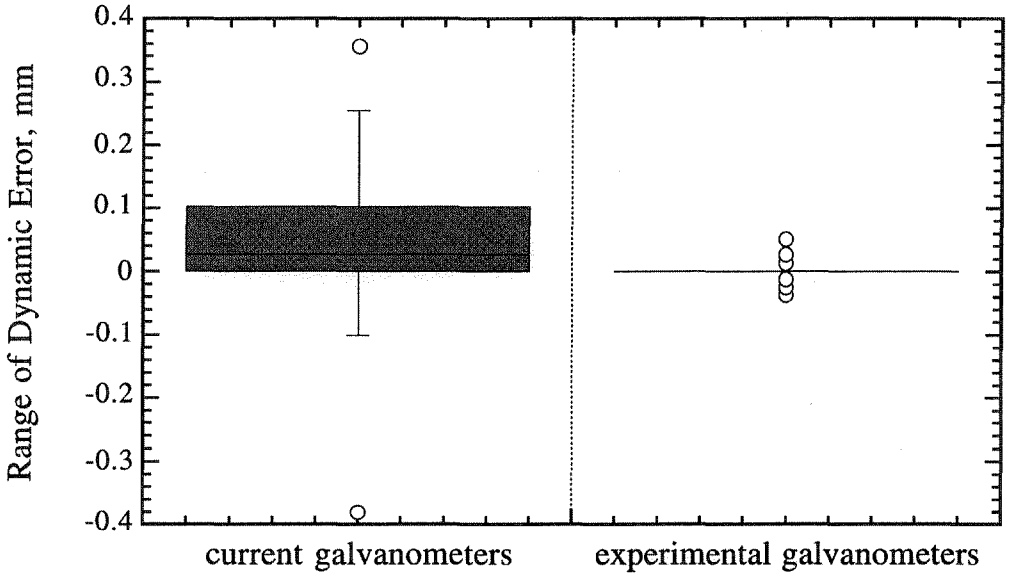

Figure 2. Dynamic errors of the current and experimental galvanometers. Errors were measured along the x and y axes across a 12 inch area.

3.1.2 Scanner Repeatability Scanner repeatability is a measure of how accurately the galvanometers can return to a given location in the build area. The repeatability specification for the current galvanometers is 120 μrad. In the Sinterstation 2000, where the distance from the galvanometers to the build plane is approximately 616 millimeters, the galvanometers are

repeatable to within 0.076 millimeters (0.003 inches). The experimental galvanometers have a repeatability specification of 10 μrad, or 0.006 millimeters (0.00024 inches) at the build plane.

Scanner repeatability dictates how well the ends of the scan vectors drawn on the build plane are aligned; the alignment of the vectors affects the smoothness of vertical surfaces. The combined effects of the scanner dynamics and scanner repeatability influence overall SLS part accuracy. There is a significant improvement in part accuracy when the new galvanometers are used to build and accuracy benchmark part in a polymer coated metal material as shown in Figure 3. This material has essentially zero shrinkage in the SLS process.

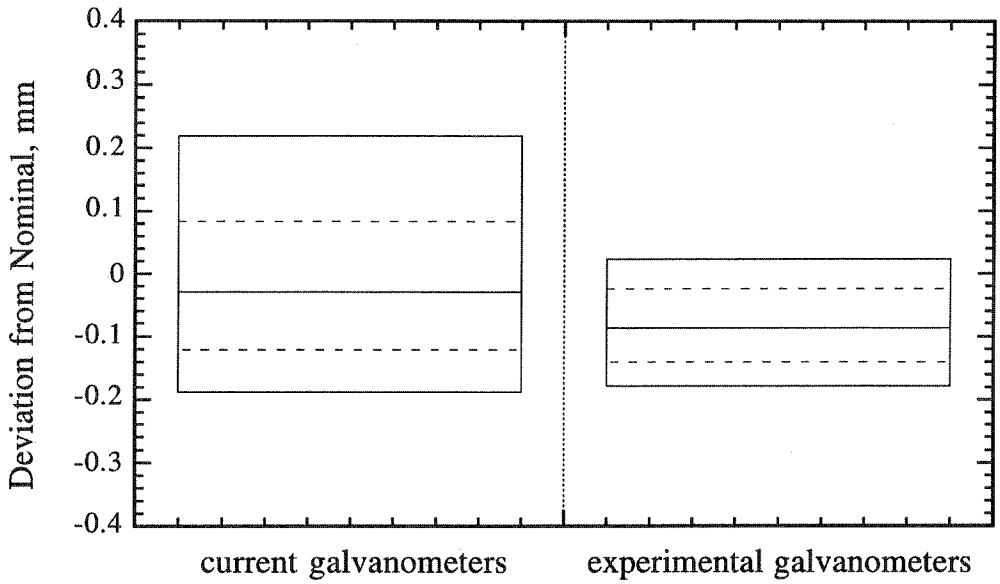

Figure 3. Error distribution for an accuracy part made using polymer coated metal material. The solid box contains 90% of the data, and the dashed box contains 50% of the data. There are 46 distinct x and y measurements in each data set.

The initial evaluation of the experimental galvanometers on different SLS machines at different sites began in May 1995. The evaluation included two builds with the current galvanometers, a retrofit of the scanner system, and the same two builds with the experimental galvanometers. The first build contained 8 parts representing a range of part geometries. These parts were built only once with each set of galvanometers to show the first time build accuracy. Also, the scale and beam offset values, calculated especially for the SLS machine and material, were applied to all of the STL files in the build packet.

Preliminary results of the evaluation program are presented in Table 1. Parts built with the experimental galvanometers show less random error than parts built with the current galvanometers. The range of error is reduced by approximately 25 to 35% to a value of ± 0.25 mm for nylon and polycarbonate, while the range of error is reduced by approximately 40 to 50% to a value of ± 0.10 mm for metals. The different range of error values for the polymers and

coated metal material can be attributed to some of the materials issues discussed earlier. Parts made from the polymers experience errors associated with thermal variability, shrinkage as well as beam positioning. Parts made with the polymer coated metal system, however, are only affected by beam positioning errors since the material is processed at ambient temperature and there is essentially no density change associated with the laser processing.

Table 1. Summary of accuracy measurements from the multiple site evaluation of the experimental galvanometers. The part build contained 8 parts representing a range of geometries. The range of error includes 90% of the measured dimensions.

Site	Material	Current galvanometers millimeters (inches)	Experimental galvanometers millimeters (inches)	Improvement
#1	polymer coated metal	± 0.201 mm (± 0.0079 inches)	± 0.102 (± 0.0040)	49.3 %
#2	polycarbonate (LPC 3000)	± 0.424 (± 0.0167)	± 0.284 (± 0.0112)	33.0 %
#3	polycarbonate (LPC 3000)	± 0.381 (± 0.0150)	± 0.246 (± 0.0097)	35.4 %
#4	polycarbonate (LPC 3000)	± 0.376 (± 0.0148)	± 0.257 (± 0.0101)	31.6 %
#1	fine nylon (LFN 5000)	± 0.414 (± 0.0163)	± 0.310 (± 0.0122)	25.1 %

3.1.3 Parameter Tuning The scanner parameters used with the experimental galvanometers are being optimized to increase dimensional accuracy of the scanned regions. The optimization is focused on the Laser On (LO) and the Laser Off (LF) parameters (13). The Laser On command compensates for the initial delay caused by the inertia of the fast axis mirror and rotor. When the scanner controller sends a ramp signal to the galvanometer, telling it to change position, there is a finite delay before the galvanometer starts to move, as is shown in Figure 4a. Because the galvanometer system does not have position feedback to the controller, the controller sends the ramp signal to the galvanometer then waits for a time interval to elapse, specified by the LO parameter, before turning the laser ON.

At the end of the vector scan, the scanner still lags the ramp signal by some amount and requires time to reach the actual endpoint of the drawn vector. The Laser Off delay allows the scanner to reach the end of the drawn vector before the laser is turned off. In Figure 4b, the ramp signal is sent to the galvanometers at time equal zero, but the galvanometers do not reach their final position until approximately 1500 μs have elapsed. The time interval specified by the Laser Off parameter starts when the stop command is sent to the galvanometer.

The optimal set of LO and LF parameters are a function of the scan speed. As the scan speed increases, the Laser On and Laser Off delays decrease because the galvanometers accelerate/decelerate more rapidly. To optimize the parameters, high and low values are chosen for the LO and LF, then a designed experiment using a structured set of permutations of these parameters is used to build SLS parts. The SLS parts are then measured, and the optimal set of LO/LF parameters are calculated on the basis of part accuracy, repeatability, surface finish, and eccentricity.

An appropriate range of LO and LF values can be found by scanning a position sensitive detector (PSD) and plotting the galvanometer position as a function of time, Figure 4. Data collection is initiated when a move signal is sent to the galvanometers, and thus the LO and LF delays can be directly related to the ordinate of the graph. Using the data in Figure 4, at a Step Size of 80, the initial range of values used for the LO and LF were 700 to 1300μs and 1100 to 1700μs, respectively.

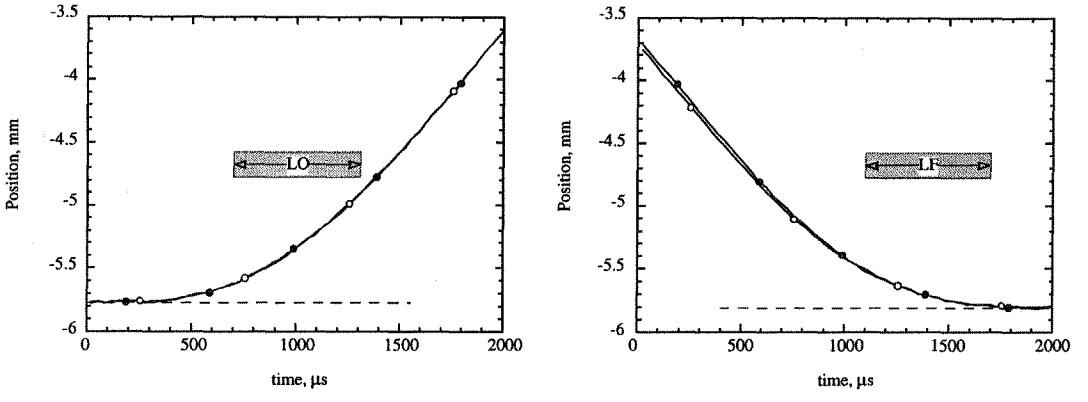

Figure 4. Galvanometer position as a function of time (left: acceleration curve; right: deceleration curve). The galvanometer is moving at a Step Size (SS) of 80 LSB's. A move signal is sent to the galvanometers at time equal zero. Legend: ○ 100 mm vector, ● 10 mm vector.

3.2 Scale/Offset Calibration and Compensation As discussed in Section 2.2, there are dimensional changes associated with material shrinkage and growth during the fabrication of the SLS object. Software is available to compensate for these effects, given the proper scale and offset values. DTM has recently revised the procedure to calculate scale and offset values for each of the Laserite materials. The new scale/offset procedure includes the building and measurement of parts, Figure 5, that contain nominal dimensions ranging from 5 to 178 mm (0.2 to 7.0 inches). The deviation from the nominal for each dimension is plotted versus the nominal dimension, and the best linear fit is drawn through the data. The slope of the line is the shrinkage (or expansion) value. A negative slope corresponds to a shrinkage value. The scale value required to compensate for the shrinkage is equal to 1/(1-shrink). The intercept of the line is twice the beam offset value ($2d$), because all of the dimensions are measured on outward facing surfaces. The beam compensation software moves the skin (or surface) of the STL file inward a specified distance, d.

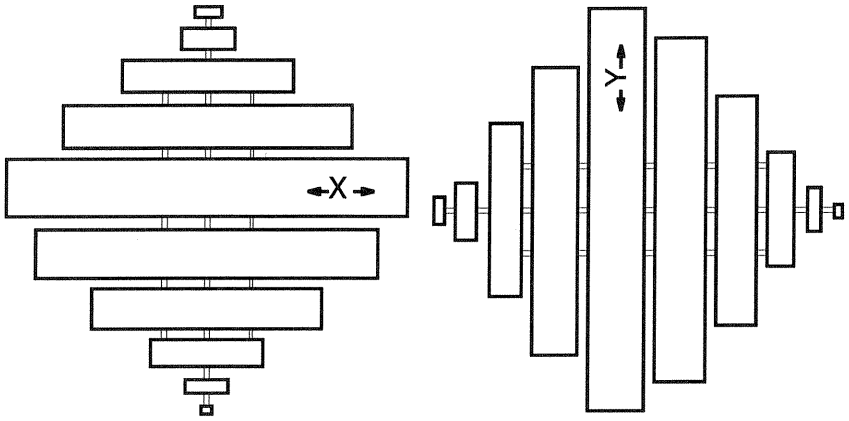

Figure 5. Parts built and measured to calculate scale and offset values for the polymer materials used in the Sinterstation 2000 System.

The current methods of beam compensation include normal offset and constant offset. Of these two methods, the normal offset method provides the most uniform results. In the normal offset method, a vector normal is calculated at each vertex based on the normals of the adjacent facets. The vertex is moved along the vertex normal to the new offset position. This method works best for STL files that have circular and flat surfaces because the angle between the facets is large. As the angle between the facets decreases, the distance that the vertex is moved by the normal offset method is not sufficient to move the surface of the STL file by the desired amount. The constant offset method works best for square features. In this method, the vertex is offset by moving first in the x direction, then in the y direction, by the beam offset value, Figure 6c.

A new method of beam compensation, dihedral offset, is being added to the geometry tools software provided by DTM Corporation. The new method, dihedral offset, uses the dihedral angle between connecting facets to calculate the new offset position of the vertex. This method adjusts for the geometry of the part, making the dihedral offset method more accurate than the normal offset and constant offset methods. As an example, Figure 6 shows how two facets and their common vertex are offset a specific distance, *d*, using each of the three methods.

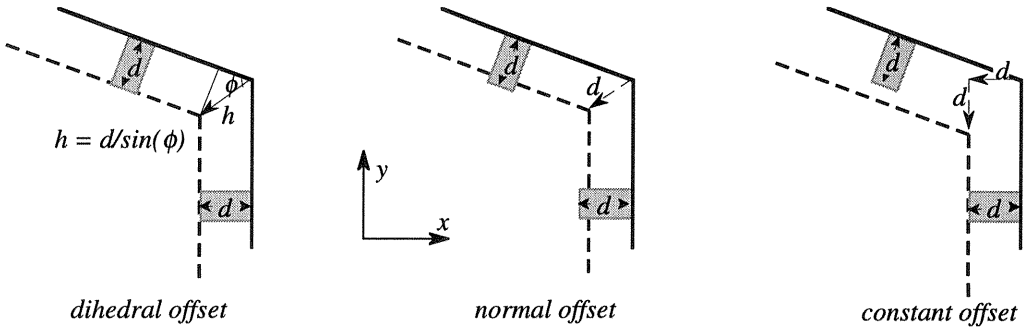

Figure 6. A visual comparison of the three offset methods available to compensate of the laser beam width. The solid line is the initial position, the dashed line is the final position, the shaded boxes represent the desired amount of offset for each facet.

3.3 Particle Size and Shape Control Process resolution is the number of distinguishable volume elements per unit volume. For SLS technology, process resolution is proportional to the inverse of the particle diameter cubed. As a result, resolution increases substantially as particle size is reduced. Parts made with smaller particles have improved definition as characterized by the sharpness of edges and corners; visually these parts are more representative of the CAD models. The impact of particle shape is more subtle but, in general, parts built with spherical particles have improved definition compared to parts build with irregular particles. This is particularly true for materials which undergo limited densification and melting in the SLS process. For such materials, particle shape is not greatly altered in the SLS process.

Initial SLS materials - wax (LW 2010), polycarbonate (LPC 3000), and nylon (LN 4010) - had mean volume average particle diameters of approximately 100 μm. The shape of both the polycarbonate and nylon particles is somewhat irregular. In 1994, a nylon material with a particle size of 50 μm was introduced. Parts produced with this material were found to have greatly improved feature resolution and definition than those produced with the coarser powders. Currently, a number of candidate material systems with small spherical particles are being examined. An example of a part made with such a powder is shown in Figure 7. The other two parts in the photo are made with coarser particles. While the three parts are made from different chemistries, they all have a similar extent of densification.

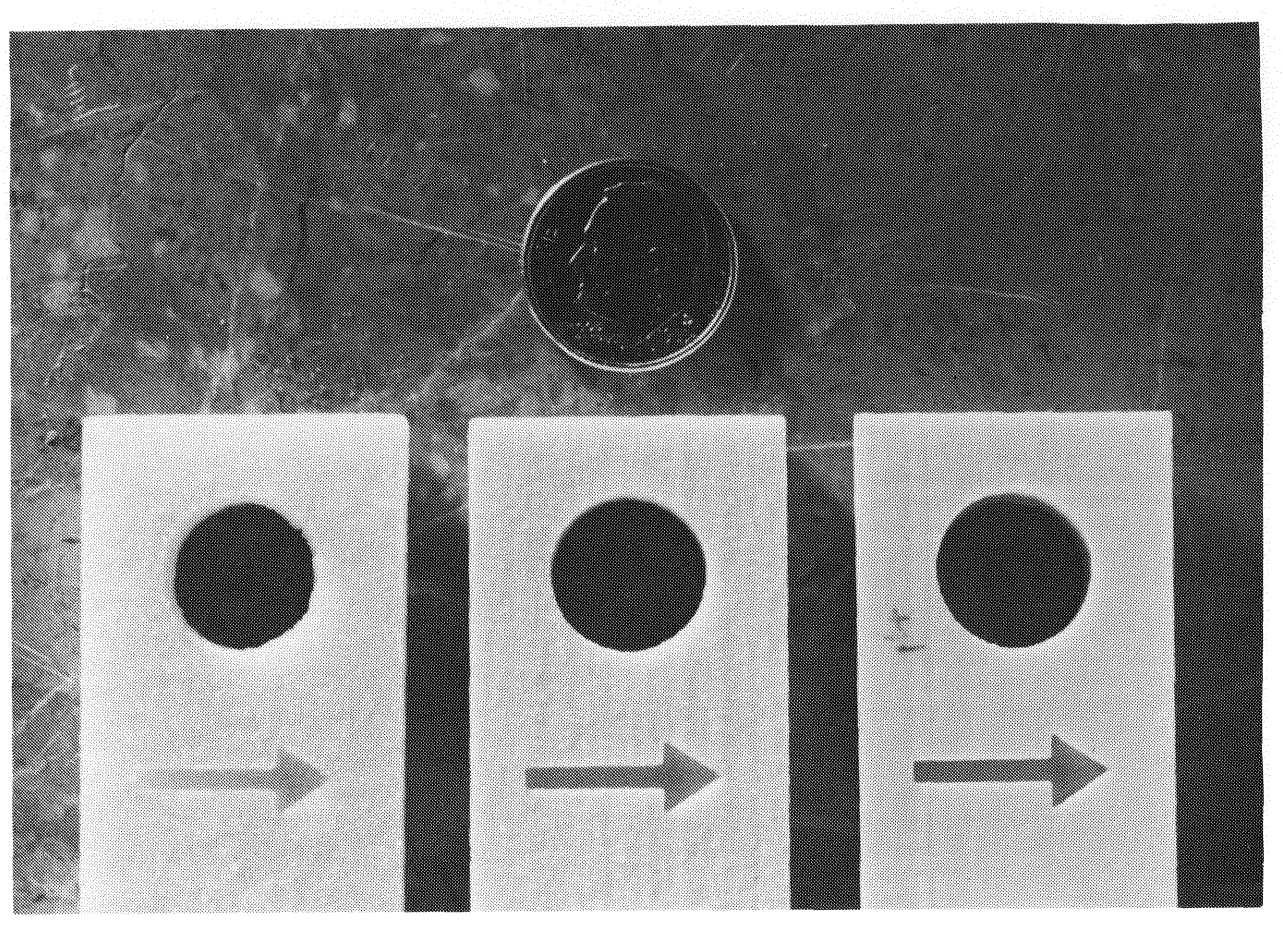

Figure 7. The reduction of particle size increases the resolution of the SLS process. The particle size decreases from left to right in the SLS parts shown.

4. CONCLUSIONS

SLS part accuracy is being improved through a series of projects. In particular, improvements to the beam delivery system, scale/offset calibration and software, and materials have been made or are in development. These improvements are summarized below:

- Dynamic scanning errors and scanner repeatability errors can be reduced by an order of magnitude with improved galvanometers.

- With the new galvanometers, the range of dimensional error is reduced by approximately 25 - 30% to ± 0.25 mm for nylon and polycarbonate, while the range of error is reduced by 40 - 50% to a value of ± 0.10 mm for polymer coated metals.

- Optimization of the scanner parameters is ongoing to improve accuracy, surface finish, and repeatability.

- The revised scale/offset calibration procedure and dihedral beam offset method provides more accurate measurement and compensation for shrinkage and laser beam width.

- Materials with controlled particle size and shape can produce parts with resolution and definition approaching that of those made with liquid-based processes.

5. REFERENCES

1. E.P. Gargiulo and D. Belfiore, "Stereolithography Process Accuracy: User Experience", Proceedings of the Second International Conference on Rapid Prototyping, University of Dayton, Dayton, Ohio, p. 311, June 1994.

2. T.H. Pang, "Stereolithography Epoxy Resins SL 5170 and SL 5180: Accuracy, Dimensional Stability, and Mechanical Properties", Proceeding of the Solid Freeform Fabrication Symposium, The University of Texas at Austin, Austin, Texas, p. 204, 1994.

3. N.P. Juster and T.H.C. Childs, "A Comparison of Rapid Prototyping Processes", Proceedings of the 3rd European Conference on Rapid Prototyping and Manufacturing, University of Nottingham, Nottingham, United Kingdom, 1994.

4. M.D. Baldwin, C. Atwood, and M.C. Maguire, "Integration of Rapid Prototyping into Investment Casting", Proceedings of the Rapid Prototyping & Manufacturing '95 Conference, Dearborn, Michigan, May 1995.

5. D. Jayaram, Benchmarking of Rapid Prototyping Systems - Beginning to Set Standards, Master's thesis, Clemson University, 1994.

6. L.D. Schmidt, "Process Performance Study of Commercially Produced Rapid Prototyping Systems", Proceedings of the Rapid Prototyping & Manufacturing '95 Conference, Dearborn, Michigan, May 1995.

7. P. Forderhase, K. McAlea, M. Michalewicz, M. Ganninger, and K. Firestone, "SLS Prototypes from Nylon", Proceeding of the Solid Freeform Fabrication Symposium, The University of Texas at Austin, Austin, Texas, p. 102, 1994.

8. K. McAlea, R. Booth, P. Forderhase, and U. Lakshminarayan, "Materials for Selective Laser Sintering Processing", Proceedings of the 1995 SAMPE Conference, 1995.

9. K. McAlea, P. Forderhase, and R. Booth, "The Development of a SLS Composite Material", Proceeding of the Solid Freeform Fabrication Symposium, The University of Texas at Austin, Austin, Texas, 1995.

10. U. Lakshminarayan, K. McAlea, D. Girouard, and R. Booth, "Manufacture of Iron-Copper Composite Parts using Selective Laser Sintering", 1995 International Conference of Powder Metallurgy and Particulate Materials, Seattle, Washington, 1995.

11. P. Forderhase, M. Ganninger, and K. McAlea, "Nylon and Nylon Composite SLS Prototypes", Proceedings of the 4th European Conference on Rapid Prototyping and Manufacturing, The University of Nottingham, Nottingham, United Kingdom, 1995.

12. J.A. Benda, Temperature-Controlled Selective Laser Sintering, Proceeding of the Solid Freeform Fabrication Symposium, The University of Texas at Austin, Austin, Texas, p. 277, 1994.

13. DG Series: Scan Head Controllers, User Manual, General Scanning, Inc., Waterton, Massachusetts, GSI PN 12P-DG, Rev #5, March, 1988.